

Model of Laser-Induced Deposition on Semiconductors from Liquid Electrolytes

Z. C. Wu[†]

*Department of Physics and Astronomy, State University of New York at Buffalo,
Buffalo New York 14260*

Daniel A. Jelski

*Department of Chemistry, State University of New York, College at Fredonia,
Fredonia, New York 14063*

Thomas F. George*

*Departments of Physics and Astronomy and Chemistry, 239 Franczak Hall,
State University of New York at Buffalo, Buffalo, New York 14260*

L. Nánai and I. Hevesi

Department of Experimental Physics, JATE, H-6720 Szeged, Hungary

F. V. Bunkin, B. S. Luk'yanchuk, M. R. Brook, and G. A. Shafeev

General Physics Institute AN SSR, SU-117942 Moscow, USSR

Received October 17, 1988

A model for laser-induced electrolytic deposition on a semiconductor surface is developed. The laser induces two effects in the surface: thermal heating, which results in a thermal potential, and the Dember effect, in which excited electrons and holes diffuse at different rates. The model is compared with experiment, and the ring-shaped deposit discovered is reproduced in the calculation.

I. Introduction

In a previous paper¹ presented experimental results of laser-induced deposition on a semiconductor surface from an electrolyte solution. CuSO_4 and $\text{KAu}(\text{CN})_2$ were dissolved in aqueous solution above a Si or GaAs surface. A copper vapor laser ($\lambda = 510.6$ nm, $f = 10$ kHz, $\tau_{\text{pulse}} = 20$ ns) illuminated the surface. This caused the deposition of copper or gold onto the surface of the semiconductor. In the early stages of the deposition process, the deposit was a ring shape which was subsequently filled in later in the process. In this paper we develop a theoretical model for the deposition process, especially its early stages. It is hypothesized that the total effect is the sum of two constituent parts, those being a thermal component and the Dember component.² These together cause an electromotive potential between the dark and illuminated areas of the surface, and this in turn creates a current through the solution.

The goal of this effort is to verify the above hypothesis and to better understand the relationship between the thermal and Dember effects. To this end, we have used a series of coupled differential equations to describe the coupling between temperature and potential and also the behavior of the nonequilibrium carriers resulting from the Dember effect. We then assume that the surface acts as a battery and thus induces a current in the neighboring solution. This results in a cathodic reaction in the dark area and an anodic reaction in the illuminated area, yielding the experimentally observed deposited ring. Thus the laser produces both the anode and the cathode for the reaction.

As mentioned in our previous paper,¹ there has been considerable effort devoted to laser-induced microchem-

istry. Gaseous deposition has been well studied,³⁻⁶ and some theoretical work has also been done.^{7,8} Deposition from liquid phases is also known.⁹⁻¹¹ The present calculation differs from these significantly, since here the laser is used to generate the potential necessary for an electrolytic reaction.

Light-induced electrolyte deposition is well documented in the literature. Early work includes the nucleation of palladium clusters on photosensitive TiO_2 films.¹² Yoneyama et al.¹³ irradiated one side of a thin TiO_2 wafer and reported the deposition of palladium onto the dark surface from a $\text{Pd}(\text{NO}_3)_2$ solution. Kobayashi et al.¹⁴ deposited ruthenium oxide and platinum on the illuminated and dark sides of a TiO_2 crystal, respectively. Finally, palladium films were deposited on TiO_2 surfaces by millisecond UV illumination.¹⁵

(1) Nánai, L.; Hevesi, I.; Bunkin, F. V.; Luk'yanchuk, B. S.; Brook, M. F.; Shafeev, G. A.; Jelski, D. A.; Wu, Z. C.; George, T. F. *Appl. Phys. Lett.* **1989**, *54*, 736.

(2) Seeger, K. *Semiconductor Physics: An Introduction*; Springer-Verlag: Berlin, 1982; pp 145-146.

(3) Brueck, S. R. J.; Ehrlich, D. J. *Phys. Rev. Lett.* **1982**, *48*, 1678.

(4) Ehrlich, D. J.; Osgood, R. M.; Deutsch, T. F. *Appl. Phys. Lett.* **1980**, *36*, 698.

(5) Ehrlich, D. J.; Osgood, R. M.; Deutsch, T. F. *Appl. Phys. Lett.* **1981**, *38*, 946.

(6) von Gutfeld, R. J.; Tynan, E. E.; Melcher, R. L.; Blum, S. E. *Appl. Phys. Lett.* **1979**, *35*, 651.

(7) Jelski, D. A.; George, T. F. *J. Appl. Phys.* **1982**, *61*, 2353.

(8) Moylan, C. R.; Baum, T. H.; Jones, C. R. *Appl. Phys. A* **1986**, *40*, 1.

(9) Alferov, Zh. I.; Goryachev, D. N.; Gurevich, S. A.; Misero, M. N.; Portner, E. L.; Ryykin, B. S. *Sov. Phys. Technol. Phys.* **1976**, *21*, 857.

(10) Osgood, R. M.; Sanchez-Rubis, A.; Ehrlich, D. J.; Daneu, V. *Appl. Phys. Lett.* **1982**, *40*, 391.

(11) Bunkin, F. V.; Luk'yanchuk, B. S.; Shafeev, G. A.; Kozlova, G. A.; Portniagin, A. I.; Yeryomenko, A. A.; Mogyrosi, P.; Kiss, I. G. *Appl. Phys. A* **1985**, *37*, 117.

(12) Kelly, J. J.; Vondeling, J. K. *J. Electrochem. Soc.* **1975**, *122*, 1103.

(13) Yoneyama, H.; Nishimura, N.; Tamura, H. *J. Phys. Chem.* **1981**, *85*, 268.

(14) Kobayashi, T.; Taniguchi, Y.; Yoneyama, H.; Tamura, H. *J. Phys. Chem.* **1983**, *87*, 768.

[†] Present address: Department of Chemistry, University of Kansas, Lawrence, KS 66045.

* Author to whom correspondence should be addressed.

More relevant to the present work is the photochemical deposition of metals onto p-silicon.¹⁶ Electron-hole pairs are photogenerated, and the electrochemical reaction occurs as a result of an externally applied potential. By masking the light source, deposition in any arbitrary pattern can be accomplished. Similarly,¹⁷ instead of application of an external potential, a metal anode is placed in contact with the silicon wafer some distance away from the area to be plated. The cathodic reaction then occurs as above. Reversible imaging techniques, using photoelectrochemistry, have also been of interest.¹⁸ Finally, Bunkin et al.¹⁹ have measured the temperature distribution of temperature and charge in a laser-heated electrolyte.

Early theory was developed by Möllers et al.²⁰ in a paper concerned with the origin of the photocatalytic effect. This work was continued by Memming.²¹ It is useful to distinguish between processes requiring electrodes and the so-called electroless processes. The present work is concerned with the electroless process, i.e., no external potential is required for the reaction to proceed. The advantage, of course, is experimental simplicity and flexibility. The electroless process depends only on the laser-induced potential for the redox reaction.

In section II we present the theory behind the calculation. In section III we justify the various approximations made. These approximations also yield some physical insight and therefore constitute part of our result. We also present our numerical data and compare them with experiment. Section IV contains a brief summary.

II. Theory

The laser-induced electric potential at a semiconductor surface depends on two effects: the thermoelectric effect and the Dember effect. The corresponding thermal emf and Dember photon emf are of the same order of magnitude. We shall discuss these two effects separately in what follows.

With respect to the thermal emf, we can temporarily ignore the electron-hole pair production induced by the laser beam and consider the laser simply as a heating device. In the bulk, we can consider each point to be in local thermal equilibrium, but there is a macroscopic temperature gradient caused by the absorption of energy from the laser beam. The equation of entropy conservation is

$$\frac{\partial S}{\partial t} + \bar{\nabla} \bar{J}_s = \frac{1}{T} P_s \quad (1)$$

where S is the entropy density, \bar{J}_s is the entropy flux, and P_s is the heat absorption rate per volume

$$P_s = 2\alpha P_0 e^{-2\alpha z} \quad (2)$$

where P_0 is the laser power and α is the absorptivity. The depth from the surface is represented by z . We assume the laser beam to be vertical to the surface, and the laser energy will eventually become heat.

Since we are presently ignoring the nonequilibrium carriers (created pairs), we can assume that there exist

linear relations between the currents and the generalized forces and that the relations are valid near equilibrium. These are

$$\bar{J}_s = -L_{ss} \bar{\nabla} T - L_{se} \bar{\nabla} \mu_e - L_{sh} \bar{\nabla} \mu_h \quad (3)$$

$$\bar{J}_e = -L_{es} \bar{\nabla} T - L_{ee} \bar{\nabla} \mu_e - L_{eh} \bar{\nabla} \mu_h \quad (4)$$

$$\bar{J}_h = -L_{hs} \bar{\nabla} T - L_{he} \bar{\nabla} \mu_e - L_{hh} \bar{\nabla} \mu_h \quad (5)$$

where the coefficients L_{mn} must satisfy the Onsager reciprocal relation²²

$$L_{mn} = L_{nm} \quad (6)$$

with $L_{ss} = K/T$, where T is the temperature, K is the coefficient of thermal conductivity, and μ_e and μ_h are the chemical potential of electrons and holes, respectively. We also suppose that the Coulomb term dominates (i.e., the mean free path is very short), so that the gradients of the chemical potentials can be written as

$$\bar{\nabla} \mu_e = e\bar{E} \quad (7)$$

$$\bar{\nabla} \mu_h = -e\bar{E} \quad (8)$$

where \bar{E} is the electric field.

Under the condition of zero current, the thermal potential is derived as

$$U_{\text{thermal}} = \int_l \frac{(L_{hs} - L_{es}) \bar{\nabla} T}{e(2L_{he} - L_{ee} - L_{hh})} dl \quad (9)$$

where l represents a closed loop. If the surface is entirely within a region where the coefficients L_{mn} are constant, then U_{thermal} is identically zero. The thermal potential on the surface is proportional to the temperature difference along it. If, as turns out to be the case, the evolution of the temperature is essentially independent of the evolution of the charge carriers, then the temperature can be calculated simply by solving the diffusion equation

$$C \frac{\partial T}{\partial t} = K \nabla^2 T + P_s \quad (10)$$

where C is the heat capacity and K is the heat conductivity of the semiconductor.

Now we consider the Dember effect, which is due to the different mobilities of electrons and holes and also to the pair production of local, nonequilibrium carriers, $\delta\rho_e$ and $\delta\rho_h$. These must obey the diffusion equations

$$\frac{\partial \delta\rho_e}{\partial t} = D_e \nabla^2 \delta\rho_e + P - \frac{1}{\tau} \delta\rho_e \quad (11)$$

$$\frac{\partial \delta\rho_h}{\partial t} = D_h \nabla^2 \delta\rho_h + P - \frac{1}{\tau} \delta\rho_h \quad (12)$$

where P is the pair production rate, τ is the lifetime of the created pair, and D_h and D_e are the diffusion constants for holes and electrons, respectively. The pair lifetime is on the order of 0.01 s and is thus very long on the time scale of this problem. Thus the last term will be neglected, in which we can readily calculate the Dember emf as

$$U_{\text{Dember}} = \int_l \frac{D_e \bar{\nabla} \delta\rho_e - D_h \bar{\nabla} \delta\rho_h}{e(L_{ee} + L_{hh} - 2L_{eh})} dl \quad (13)$$

We can get the Dember potential along the surface simply from $\delta\rho_e$ and $\delta\rho_h$, provided all coefficients in (13) are constant.

The local deposition rate on the surface is equivalent to the normal component of the electric current across

(15) Jacobs, J. W. M. *J. Phys. Chem.* **1986**, *90*, 6507.
 (16) Rose, T. L.; Longendorfer, D. H.; Rauh, R. D. *Appl. Phys. Lett.* **1983**, *42*, 193.
 (17) Micheels, R. H.; Darrow, A. D., II; Rauh, R. D. *Appl. Phys. Lett.* **1981**, *39*, 418.
 (18) Inoue, T.; Fujishima, A.; Honda, K. *J. Electrochem. Soc.* **1980**, *127*, 1582.
 (19) Bunkin, N. F.; Dmitriyev, A. K.; Luk'yanchuk, B. S.; Shafeev, G. A. *Appl. Phys. A* **1986**, *40*, 159.
 (20) Möllers, F.; Tolle, H. J.; Memming, R. *J. Electrochem. Soc.* **1974**, *121*, 1160.
 (21) Memming, R. *J. Electrochem. Soc.* **1978**, *125*, 117.

(22) Onsager, L. *Phys. Rev.* **1930**, *37*, 405; *Phys. Rev.* **1931**, *38*, 2265.

Table I

quantity	symbol	value
diffusion constant, electrons	D_e	40 cm ² /s
diffusion constant, holes	D_h	10 cm ² /s
heat conductivity of semiconductor	K	10 ⁷ erg/(cm·s)
heat capacity of semiconductor	C	10 ⁸ erg/(K·mol)
laser intensity	P_0	0.01 mW
pair production rate	P	10 ²¹ s ⁻¹

semiconductor-electrolyte interface. Thus the problem reduces to calculating the current distribution at the surface. Since the electrical conductivity of a 1 M electrolyte solution is typically about 10³ Ω⁻¹ cm⁻¹ compared to a value of 10⁷ Ω⁻¹ cm⁻¹ for an n-type bulk semiconductor, as a first approximation we can ignore the presence of the electrolyte and treat the laser-irradiated surface as a battery. Given the electrical potential at the surface, we can now calculate the current distribution in the electrolyte.

The total potential is $V = U_{\text{thermal}} + U_{\text{Dember}}$, which forms the boundary condition for solving the Laplace equation in the electrolyte. We assume the conductivity of the electrolyte is constant and small and that far from the surface and the laser focal point, the potential must tend toward a constant. Hence we can find the normal component of the electric field above the semiconductor surface by taking the normal gradient, so that Ohm's law can be used to calculate the normal current.

III. Results

A certain difficulty is encountered in choosing the parameters to use in reproducing the experimental data. In most cases, the data were estimated from a standard text,²³ by using values typical for semiconductors, and also from our experimental work.¹ In many cases we make only an order of magnitude estimate, and so the qualitative nature of our results must be seen in that light.

Another difficulty was the stability condition of the differential equation.²⁴ For time steps of 1 ns, we were constrained to use a length step of 4.5×10^{-4} cm. This is much too large to accurately reproduce the experiment in which the focal point size was 1–10 μm. Since the length scale is proportional to the square root of the time step, to reproduce the experimental scale we would have to increase the number of time steps by 2 orders of magnitude. This is computationally inconvenient, and thus we have used a focal point size approximately 10 times that of the experiment.

Finally, since the laser intensity is a function of focal point size, we found that to accommodate our larger focal points, we had to decrease the laser intensity. All other parameters were estimated as closely as possible to experimental conditions. The pair production rate was chosen to match the experimentally observed potentials. The parameters we used are listed in Table I.

The relevant data to match from the experiment are a temperature gradient of 20 K from the center of the spot to the outside rim. Further, it is supposed that the Dember effect and the thermal effect yield potentials of about the same order of magnitude. Because the experiment takes place on an n-doped semiconductor, it may be assumed that the concentration of holes is very small compared to the number of electrons. For this reason, all parameters proportional to the hole population may be taken as zero,

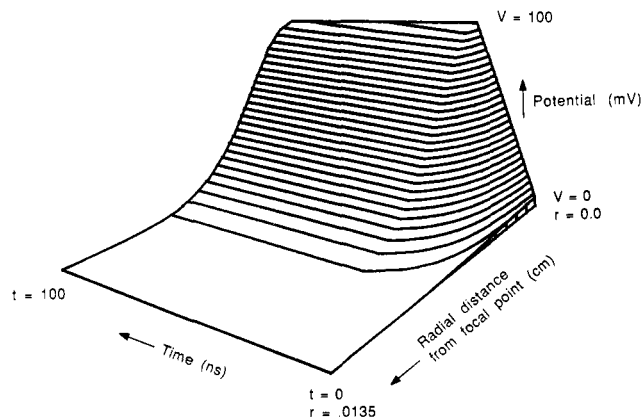


Figure 1. Illustration of the thermal potential, in millivolts. Note the slow decay of the potential after the laser is turned off.

including L_{hh} , L_{he} , and L_{hs} . Under this circumstance, eq 9 becomes

$$U_{\text{thermal}} = L_{ee} \Delta T / (eL_{ee}) \quad (14)$$

and eq 13 becomes

$$U_{\text{Dember}} = (D_e \Delta \delta \rho_e - D_h \Delta \delta \rho_h) / (eL_{ee}) \quad (15)$$

Both eq 14 and 15 are evaluated across the surface of the semiconductor.

From the experimental result of $\Delta T \cong 20$ K and the estimate of the thermal potential at about 80 mV, it follows that $L_{ee}/eL_{ee} \cong 4 \times 10^{-3}$ V/K. In turn, L_{ee} can be calculated from the electron mobility in the substrate, $L_{ee} = D_e n_e / K_B T$. Similarly, U_{Dember} can be calculated from eq 15 by using the same data.

We are further assuming that all the relevant physics occurs in the transient regime, i.e., within one laser pulse. This follows from the large difference in time scales between pulse length and pulse frequency. As will be illustrated, both the Dember and thermal effects die off within this time frame. Of course, any metal deposition on the surface will dramatically change the results of subsequent pulses.

The numerical method used is described as follows. The nonequilibrium charge carrier concentration was numerically solved from eq 11 and 12, while the temperature was calculated from eq 10. This is a simple diffusion equation with a source term. The results of this calculation were then inserted into eq 14 and 15. ΔT was calculated with respect to an ambient temperature (300 K), and the charge carrier concentration was assumed to be zero just outside the surface.

Figure 1 shows the thermal potential as a function of radial distance from the center of the focal point and time. The laser is on for the first 20 ns and then switched off. The thermal potential increases for the duration of the laser pulse and then decays very slowly with time. The variation of the potential with respect to radius is predictable; it declines monotonically with distance from the focal center.

Figure 2 illustrates the Dember potential, also as a function of radius and time. This increases dramatically as a function of time and then decreases even more dramatically as the laser is turned off. While the thermal potential never rises above 100 mV, we find that the Dember emf reaches almost 300 mV just before the laser is turned off. It then decays to almost zero within another 20 ns. Indeed, since the electron mobility is larger than the hole mobility, as the electrons move outside, the potential in the center becomes positive. After the laser is turned off, the holes also begin to move away from the

(23) Kittel, C. *Introduction to Solid State Physics*; Wiley: New York, 1968; Chapter 10.

(24) Smith, G. D. *Numerical Solution of Partial Differential Equations*; Oxford University Press: Oxford, 1965; p 139. See also: Wu, Z. C.; Jelski, D. A.; George, T. F. *Z. Phys. B* 1988, 73, 357.

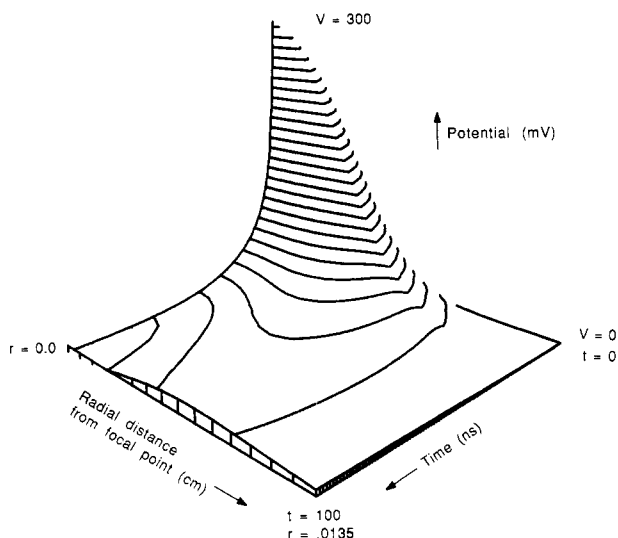


Figure 2. Illustration of the Dember potential, in millivolts. Note the rapid decay after the laser is turned off. Also note that as the holes move away from the center, a slightly negative potential at the very center appears at long times.

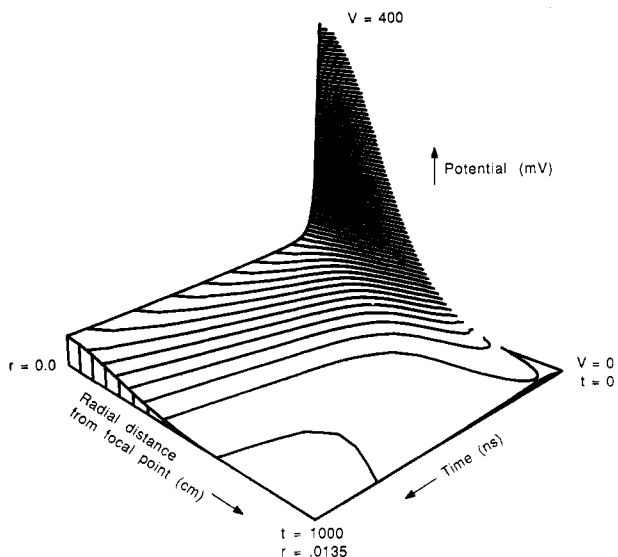


Figure 3. Illustration of the total potential, being the sum of the thermal and Dember effects. Observe that this is shown out to 1000 ns, long after the Dember effect has died away. The phenomenon is thus almost entirely due to the thermal effect.

center, and the result is that the region of maximal potential moves away from the focal point. At long times, the potential near the center becomes increasingly negative, down to about -20 mV.

Figure 3 illustrates the total potential over 1000 ns. For the duration of the laser pulse, this is dominated by the Dember potential, whereas at long times the thermal potential is the leading term. This dies away quite slowly. The time period shown is equivalent to a microsecond, but the next laser pulse occurs almost a millisecond later. At this time, even the thermal potential would be close to zero, and hence the approximation of treating each laser pulse as an independent event is justified.

The current is proportional to the space derivative of the potential. This accounts for the ring-shaped deposit structure, since it is clear that the potential must be symmetric around the focal point. The greatest variation in potential occurs directly when the laser is turned off, at which point the Dember effect is strongest and decays

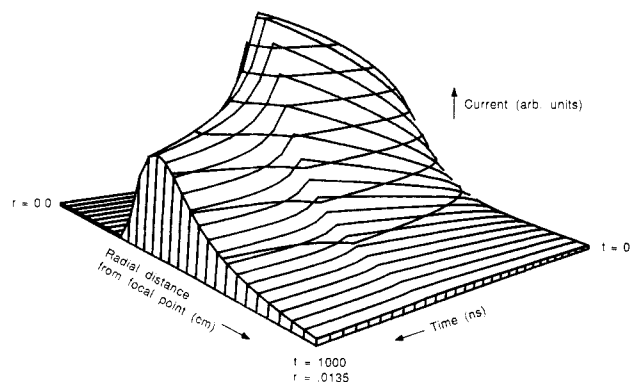


Figure 4. Representation of the deposition rate, showing positive current, i.e., where cations are flowing toward the surface. The flat region at $r = 0$ is the area where etching occurs because of the anodic reaction. The ring shape is clearly visible. While the current is strongest while the laser is still on, it remains strong even after the laser is turned off.

quickly as a function of radial distance. We suppose, however, that most deposition is a result of the thermal effect, which persists for long times and whose derivative remains relatively constant as a function of radius. Since deposition is ultimately a diffusion-limited process, the long-time behavior of the system should predominate.

Figure 4 is a graph of the actual current (except for a constant denoting the conductivity of the solution), calculated by solving the Laplace equation in a solution above the surface. This is shown for 30 ns and illustrates the effect just discussed. The flat area near $r = 0$ is the region in which the current is negative, e.g., the region in which surface etching occurs rather than deposition.

Several observations can be made. First, the deposition rate is greatest while the laser is still on. This shows that Dember effect contributes to the deposition rate, but since it falls off dramatically immediately after the laser is turned off, we suggest that the thermal effect predominates overall. Further, it may be supposed that concurrent with the Dember effect are chemical reactions on the surface, occurring as a result of the nonequilibrium electrons. Thus the moral of the story is that net deposition would be increased if the temperature differential between the irradiated and dark portions were as large as possible. For short laser pulses, the total effect of the Dember potential is small, and for longer pulses the problem of chemical rearrangement will probably become significant. Of course, we have completely neglected difficulties that might be associated with melting of the surface or other effects due to intensive heating.

IV. Summary

We have reproduced the experimental results of a laser-induced electrolytic experiment. We have shown that the ring-shaped deposition follows logically from the potential distribution induced by the laser. We have shown that both the Dember and thermal effects contribute to the process but that the thermal effect predominates because of its longlasting effect. We have demonstrated that these two effects can be treated as independent phenomena, and therefore the amount of work required in the calculation is minimized.

Acknowledgment. T.F.G. acknowledges the Office of Naval Research and the Air Force Office of Scientific Research (AFSC), United States Air Force, under Contract F49620-86-C-0009, for support of their research.